

AD-A144 373

FLUID LAYER BETWEEN INFINITE ELASTIC PLATES I
MATHEMATICS AND INTENSITY V. (U) ADMIRALTY MARINE
TECHNOLOGY ESTABLISHMENT TEDDINGTON (ENGLAND)

1/1

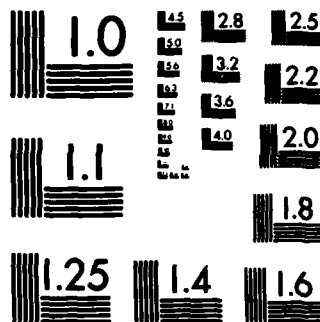
UNCLASSIFIED

J H JAMES FEB 84 AMTE(N)/TM84053

F/G 20/4

NL





MICROCOPY RESOLUTION TEST CHART
NATIONAL BUREAU OF STANDARDS-1963-A

AMTE(N)TM84053

UNLIMITED

TECH MEMO AMTE(N)TM84053

COPY No 35



ADMIRALTY MARINE TECHNOLOGY ESTABLISHMENT

AD-A144 373

FLUID LAYER BETWEEN
INFINITE ELASTIC PLATES I. MATHEMATICS
AND INTENSITY VECTORS

J. H. JAMES

DTIC FILE COPY

DTIC
ELECTED
AUG 0 8 1984

FEBRUARY 1984

UNLIMITED

099

UNLIMITED

AMTE(N)/TM84053



FLUID LAYER BETWEEN INFINITE ELASTIC PLATES I. MATHEMATICS AND INTENSITY VECTORS

BY

J.H. JAMES

Accession For	
NTIS GRA&I	<input checked="" type="checkbox"/>
DTIC TAB	<input type="checkbox"/>
Unannounced	<input type="checkbox"/>
Justification	
By	
Distribution/	
Availability Codes	
Dist	Special

A-1

Summary

→ The pressure and displacements, due to line-force and line-source excitation, are given in terms of Fourier integrals which can be evaluated numerically. Plots of intensity vectors provide a vivid illustration of the energy flow in the fluid. The selected plots show significant interchange of propagating energy between fluid and the driven plate when the excitation is a force, but not when the excitation is a source.

22 pages
11 figures

AMTE(Teddington)
Queen's Road
TEDDINGTON Middlesex TW11 0LN

February 1984

(C)

Copyright
Controller HMSO London
1984

DTIC

1. INTRODUCTION

In the absence of dissipation, the total energy flow along a uniform pipe containing a stationary fluid is conserved. However, because the system normal modes are non-orthogonal over the fluid's cross-section, the distribution of energy between the pipe's wall and the fluid need not be a constant with distance along the pipe. This interchange of energy between a pipe and its fluid is not without interest to the noise control engineer who requires to understand the physics of energy interchange between mechanical and fluid elements of a dynamic system. James [1] has given a qualitative description of the energy flow in a uniform pipe, with time-harmonic point source and force excitation, in terms of intensity vector plots in the fluid which show clearly this energy interchange. Fuller [2] has provided a quantitative description of this phenomenon by giving the mathematics, and some numerical results, of the energy distribution between pipe and fluid.

The purpose of the work described herein is to give the preliminary work necessary for a combined analytical and numerical investigation of the simpler problem of the time-harmonic line-force or line-source excitation of a system comprising of a layer of fluid bounded by two identical thin plates. This problem is much more tractable than the corresponding pipe problem, and its greater simplicity may help to clarify the physical processes that are involved in the energy interchange between fluid and plates. This initial work will give the basic mathematics needed, and also discuss some plots of acoustic intensity vectors which provide a vivid illustration of the energy flow in the fluid.

2. MATHEMATICS OF PROBLEM

The geometry of the problem is shown in Figure 1. A time-harmonic line-force or line-source drives a system comprising of a layer of fluid contained between two identical infinite elastic plates. The differential equations satisfied by the plate displacements and fluid pressure are

$$[D\partial^4/\partial x^4 - \omega^2 \rho_s h]W_1(x) = F_1 \delta(x) + p(x, H) \quad (1)$$

$$[D\partial^4/\partial x^4 - \omega^2 \rho_s h]W_2(x) = F_2 \delta(x) - p(x, 0) \quad (2).$$

$$[\partial^2/\partial z^2 + \partial^2/\partial x^2 + k^2]p(x, z) = -4\pi p_0 \delta(x) \delta(z - z_0) \quad (3)$$

where $D = Eh^3/12(1 - \sigma^2)$ is the flexural rigidity of the plates whose densities are ρ_s and whose thicknesses are h ; $W_1(x)$ and $W_2(x)$ are, respectively, the vertical displacements of the upper and lower plates; $p(x, z)$ is the acoustic pressure in the fluid layer whose density is ρ and whose sound velocity is c ; k is the acoustic wavenumber, ω/c ; F_1 and F_2 are the amplitudes of the line-forces that are applied to the upper and lower plates, respectively; p_0 is the amplitude of the line-source whose free-field pressure is given in numerous texts, for example [3], as

$$G_p(x, z) = \pi i p_0 H_0(k\sqrt{x^2 + z - z_0^2}) \quad (4)$$

in which H_0 is the Hankel function $J_0 + iY_0$; the time-harmonic factor $\exp(-i\omega t)$, is omitted throughout.

The analysis proceeds via the Fourier transform

$$\begin{bmatrix} W_1(x) \\ W_2(x) \\ p(x, z) \end{bmatrix} = (1/2\pi) \int_{-\infty}^{\infty} \begin{bmatrix} \bar{W}_1(\alpha) \\ \bar{W}_2(\alpha) \\ \bar{p}(\alpha, z) \end{bmatrix} \exp(i\alpha x) d\alpha \quad (5)$$

where

$$\begin{bmatrix} \bar{W}_1(\alpha) \\ \bar{W}_2(\alpha) \\ \bar{p}(\alpha, z) \end{bmatrix} = \int_{-\infty}^{\infty} \begin{bmatrix} W_1(x) \\ W_2(x) \\ p(x, z) \end{bmatrix} \exp(-i\alpha x) dx \quad (6)$$

The general solution of the differential equation (3) in the spectral domain is

$$\bar{p}(\alpha, z) = \bar{G}_p(\alpha, z) + \bar{p}_g(\alpha, z) \quad (7)$$

where [3]

$$\bar{G}_p(\alpha, z) = 2\pi i p_0 \gamma^{-1} \exp(i\gamma(z - z_0)), \quad z > z_0 \quad (8)$$

$$\bar{G}_p(\alpha, z) = 2\pi i p_0 \gamma^{-1} \exp(-i\gamma(z - z_0)), \quad z < z_0$$

and

$$\bar{p}_g(\alpha, z) = A(\alpha) \exp(i\gamma z) + B(\alpha) \exp(-i\gamma z)$$

in which $\gamma = \sqrt{k^2 - \alpha^2}$, and $A(\alpha)$ and $B(\alpha)$ are the unknown constants of integration of the homogeneous wave-equation.

The spectral forms of equations (1) and (2) may be written in matrix notation as

$$(\text{Da}^4 - \omega^2 \rho_s h) \begin{bmatrix} \bar{W}_1(\alpha) \\ \bar{W}_2(\alpha) \end{bmatrix} = \begin{bmatrix} F_1 \\ F_2 \end{bmatrix} + \begin{bmatrix} \bar{P}(\alpha, H) \\ -\bar{P}(\alpha, 0) \end{bmatrix} \quad (9)$$

Eliminate \bar{P} from this equation, by the use of equations (7) and (8) to give

$$(\text{Da}^4 - \omega^2 \rho_s h) \begin{bmatrix} \bar{W}_1(\alpha) \\ \bar{W}_2(\alpha) \end{bmatrix} = \begin{bmatrix} F_1 \\ F_2 \end{bmatrix} + \begin{bmatrix} \exp(i\alpha H) & \exp(-i\alpha H) \\ -1 & -1 \end{bmatrix} \begin{bmatrix} A(\alpha) \\ B(\alpha) \end{bmatrix} \quad (10)$$

$$+ 2\pi i p_0 \gamma^{-1} \begin{bmatrix} \exp(i\gamma(H-z_0)) \\ -\exp(i\gamma z_0) \end{bmatrix}$$

The boundary conditions at the interfaces require continuity of normal displacements, viz.

$$\{\partial p(x, z)/\partial z\}_{z=H} = \rho \omega^2 W_1(x) \quad (11)$$

$$\{\partial p(x, z)/\partial z\}_{z=0} = \rho \omega^2 W_2(x)$$

which give the spectral equations

$$\rho \omega^2 \begin{bmatrix} \bar{W}_1(\alpha) \\ \bar{W}_2(\alpha) \end{bmatrix} = i\gamma \begin{bmatrix} \exp(i\gamma H) & -\exp(-i\gamma H) \\ 1 & -1 \end{bmatrix} \begin{bmatrix} A(\alpha) \\ B(\alpha) \end{bmatrix} + 2\pi p_0 \begin{bmatrix} -\exp(i\gamma(H-z_0)) \\ \exp(i\gamma z_0) \end{bmatrix} \quad (12)$$

Elimination of $\bar{W}_1(\alpha)$ and $\bar{W}_2(\alpha)$ between equations (10) and (12) gives the matrix equation from which the unknowns, $A(\alpha)$ and $B(\alpha)$, may be obtained, viz.,

$$i\gamma \begin{bmatrix} D^+ \exp(i\gamma H) & -D^- \exp(-i\gamma H) \\ D^- & -D^+ \end{bmatrix} \begin{bmatrix} A(\alpha) \\ B(\alpha) \end{bmatrix} = \rho \omega^2 \begin{bmatrix} F_1 \\ F_2 \end{bmatrix} + 2\pi p_0 D^+ \begin{bmatrix} \exp(i\gamma(H-z_0)) \\ -\exp(i\gamma z_0) \end{bmatrix} \quad (13)$$

where

$$D^+ = D\alpha^4 - \omega^2 \rho_s h + i\rho\omega^2/\gamma \quad (14)$$

$$D^- = D\alpha^4 - \omega^2 \rho_s h - i\rho\omega^2/\gamma$$

The spectral pressure, $\bar{p}(\alpha, z)$, is obtained from equation (7), and the spectral displacements, $\bar{W}_1(\alpha)$ and $\bar{W}_2(\alpha)$ are obtained from equation (12). The spectral acoustic particle displacements, $\bar{W}_x(\alpha, z)$ and $\bar{W}_z(\alpha, z)$, in the horizontal and vertical directions, respectively, are given by the equations

$$\rho\omega^2 \bar{W}_x(\alpha, z) = i\alpha \bar{p}(\alpha, z) \quad (15)$$

$$\rho\omega^2 \bar{W}_z(\alpha, z) = i\gamma\{A(\alpha)\exp(i\gamma z) - B(\alpha)\exp(-i\gamma z)\} + C(z, z_0)$$

where

$$C(z, z_0) = -2\pi p_0 \exp(i\gamma(z-z_0)), \quad z > z_0 \quad (16)$$

$$C(z, z_0) = 2\pi p_0 \exp(-i\gamma(z-z_0)), \quad z < z_0$$

The displacements of the plates, and the pressure and particle displacements in the fluid, are obtained by numerical or contour integration of the Fourier integrals.

3. NUMERICAL RESULTS

The Fourier integrals of equation (4), with upper limits of integration set to approximately twice the highest free-wavenumber at the selected frequency, were evaluated by a simple adaptive Gaussian quadrature scheme. Because the integrals must be evaluated in the principal value sense, it is necessary to introduce damping into the system via a complex Young's modulus, $E(1-i\eta_s)$, and a complex sound velocity, $c(1-i\eta_f)$. The following constants in SI units were used in the computations:

$$\begin{aligned} E &= 19.5 \times 10^{10} & \sigma &= 0.29 & \rho_s &= 7700.0 & h &= 0.01 \text{ or } 0.05 \\ \rho &= 1000.0 & c &= 1500.0 & H &= 0.20 \\ \eta_s &= 0.02 & \eta_f &= 0.001 \end{aligned}$$

The chosen values of the loss-factors have little effect on the appearance of the intensity vector plots.

Some dispersion plots of the dissipation-free system are shown in Figures 2 and 3 for the cases of plate thickness of 0.01 and 0.05m, respectively. In Figure 2, the near identical branches, labelled 1 and 2, are symmetric and antisymmetric modes whose motion is mostly confined to the plates, their group velocity being approximately twice their phase velocity. The branches labelled 3-5 are predominantly fluid waves in which the phase

and group velocities at cut-on are infinity and zero, respectively; in fact, the branch labelled 3, at frequencies above 3kHz, is close to a plane-wave. In Figure 3, the branches labelled 1 and 2 start as predominantly plate waves in which the group velocity is approximately twice the phase velocity, and end as fluid waves in which the phase and group velocities are approximately equal. The branches labelled 3-5 start as fluid waves, but they also change their nature as the frequency increases. It should be kept in mind, however, that the plate theory, for the 0.05m plate, is of limited validity at frequencies above 5kHz. Crighton [4] has discussed the free-waves on a fluid loaded elastic plate and Fuller & Fahy [5] have discussed the changing nature of the wavenumber branches with frequency for the case of a fluid-filled pipe.

The components of the intensity vectors in the fluid-layer are defined as

$$I_x(x,z) = (1/2) \text{Real}[p(x,z)\dot{w}_x^*(x,z)]$$

$$I_z(x,z) = (1/2) \text{Real}[p(x,z)\dot{w}_z^*(x,z)]$$
(17)

where * denotes complex conjugate. The vector plots at selected frequencies are shown in Figures 4-11 in which the even numbered Figures are for force excitation of the lower plate, while the odd numbered Figures are for a source excitation located at $z=H/3$. Due to the symmetry of the problem, only the vectors for $x>0$ are shown; they are normalised to the same maximum length in each Figure, their individual lengths being proportional to $I^{1/2}$. Vectors are plotted only for a plate thickness of 0.01m; hence, it is Fig. 2 which shows the free-wavenumbers of the system.

In Figure 4, the interaction of the symmetric and antisymmetric plate waves (1,2) produces propagating energy flow, at distances in excess of 0.4m, which decays exponentially in the vertical direction. The circulating energy flow at 0.2m is caused by interaction of propagating modes with evanescent modes; they are a common characteristic in intensity vector plots. In Figure 5, at distances less than 0.4m, the absence of propagating fluid waves results in a dominance of non-propagating energy flow caused by interaction among evanescent modes; the weak excitation of the plate-waves (1,2) being evident at distances in excess of 0.4m.

In Figure 6, the interaction between the plate-waves (1,2) and the fluid-wave (3) results in a well-defined interchange of energy between the fluid and the lower plate; also evident in the upper-half of the layer is the fluid-wave (3), on its own, which is close to a plane-wave. In Figure 7 the fluid-wave (3) dominates the energy flow, the interaction between plate and fluid being insignificant.

The increasing complexity, with increasing frequency, of the energy flow is shown in Figures 8-11. Of particular interest is the rising and falling of the energy in the fluid; the well-defined interchange of energy between fluid and plate when the excitation is a line-force; and, the absence of significant energy interchange when the excitation is a source.

Some vector plots have also been obtained for the case of the fluid layer bounded by 0.05m plates, but they are not shown here. At 10kHz, which is above the plate 'coincidence' frequency, there is a very strong interchange of energy between the upper and lower plates. These, and other, intensity vector plots will be shown in continuation reports.

4. CONCLUDING REMARKS

Formulae have been given for the Fourier transforms of the pressure and displacements, due to time-harmonic line-force and line-source excitation. Some plots of intensity vectors show propagating energy interchange between the fluid and the force excited plate, which is a result of an interaction between propagating plate and fluid waves. Vectors due to source excitation do not show energy interchange, due, presumably, to the very weak excitation of the plate waves. The plots provide a vivid illustration of the energy flow in the fluid, their physical interpretation being greatly facilitated by the availability of wavenumber-frequency plots.

Follow-up projects should include; (a) further, but trivial, analytical work to try to obtain simple closed-form expressions for the transformed quantities of interest, for example, it is possible to obtain the dispersion relation from the determinant of equation (13) as

$$\tan(\gamma H)/\gamma + (D\alpha^4 - \omega^2 \rho_g h)/\{\gamma^2(D\alpha^4 - \omega^2 \rho_g h)^2 - \rho^2 \omega^4\} = 0; \quad (18)$$

(b) numerical evaluation of the energy distribution between fluid and plates, as a function of horizontal distance, for a variety of material and geometric constants; (c) interpretation of mathematics and numerical results to give conditions under which energy transfer between plates and fluid is of most significance; (d) investigation of the effects of line-constraints, which can be attached to the plates by the method of dynamic stiffness coupling [6]; and finally, (e) extension of the work to include the effects of plates of unequal thicknesses, with fluids rather than vacuums in the upper and lower half-spaces. Such a project, based partly on Fuller's paper [2] and the work herein, may help considerably to clarify the physics of energy flow in fluid-filled pipes.

J.H. James (PSO)

REFERENCES

1. JAMES J.H., Acoustic intensity vectors inside infinite cylindrical elastic shell, Admiralty Marine Technology Establishment, Teddington, AMTE(N)TM82103, December 1982.
2. FULLER C.R., Monopole excitation of vibrations in an infinite cylindrical elastic shell filled with fluid. Private communication from author. To be published.
3. SKELTON E.A., Free-space Green's functions of the reduced wave equation, Admiralty Marine Technology Establishment, Teddington, AMTE(N)TM82073, September 1982.
4. CRIGHTON D.G., The free and forced waves on a fluid-loaded elastic plate, J.Sound.Vib., 63(2), 1979, pages 225-235.
5. FULLER C.R., FAHY P.J., Characteristics of wave propagation and energy distribution in cylindrical elastic shells filled with fluid, J.Sound.Vib., 81(4), 1982, pages 501-508.
6. SPICER W.J., Acoustic intensity vectors from an infinite plate with line attachments, Admiralty Marine Technology Establishment, Teddington, AMTE(N)TM81086, October 1981.

REPORTS OF THE ADMIRALTY ARE NECESSARILY
AVAILABLE TO MEMBERS OF THE PUBLIC
OR TO COMMERCIAL ORGANISATIONS

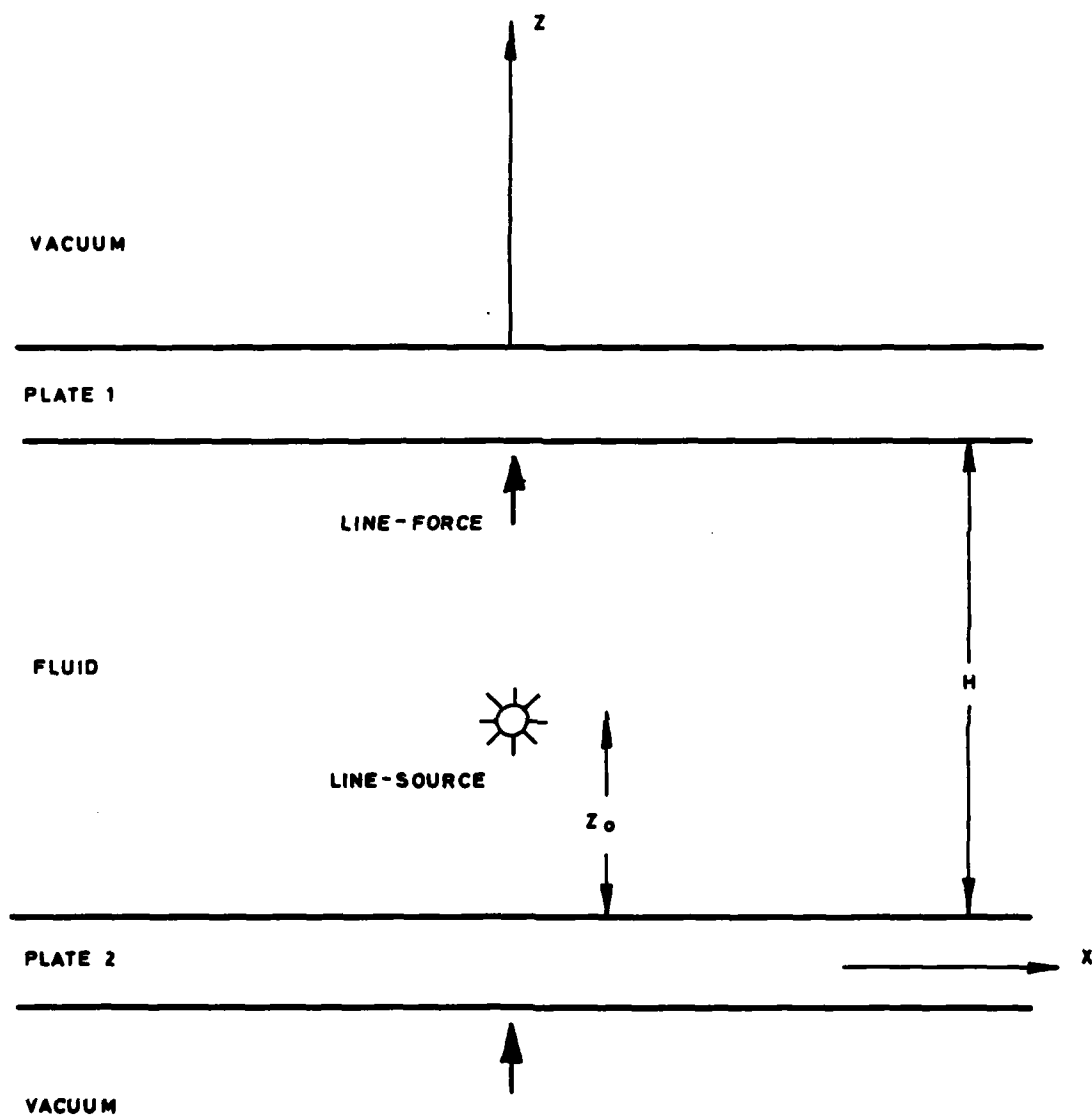


FIG. 1 GEOMETRY OF PLATE - FLUID SYSTEM

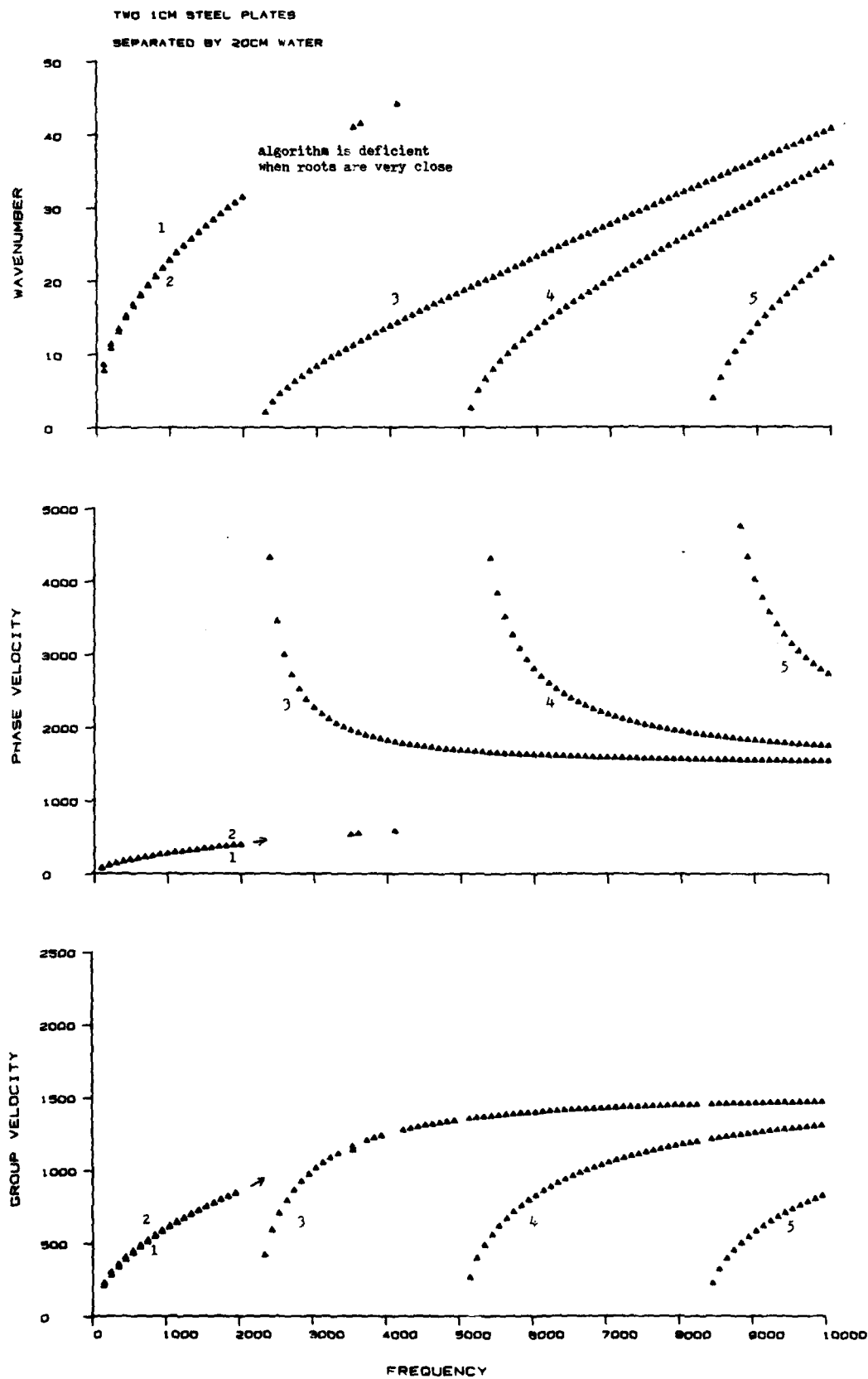


FIG.2 DISPERSION PLOTS FOR LAYER WITH 1CM PLATES

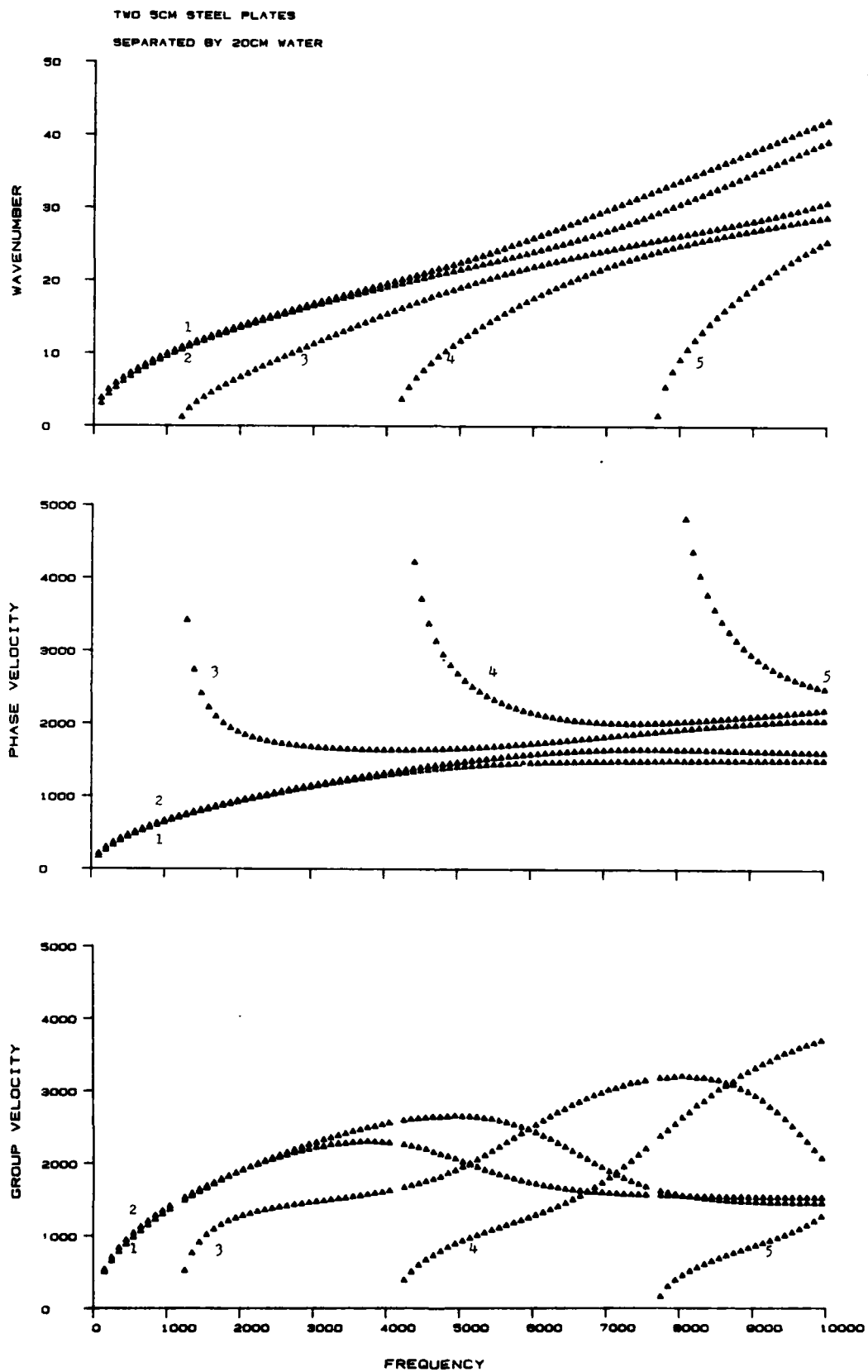


FIG.3 DISPERSION PLOTS FOR LAYER WITH 5CM PLATES

TWO 1CM STEEL PLATES SEPARATED BY 20CM WATER

FREQUENCY=1000HZ

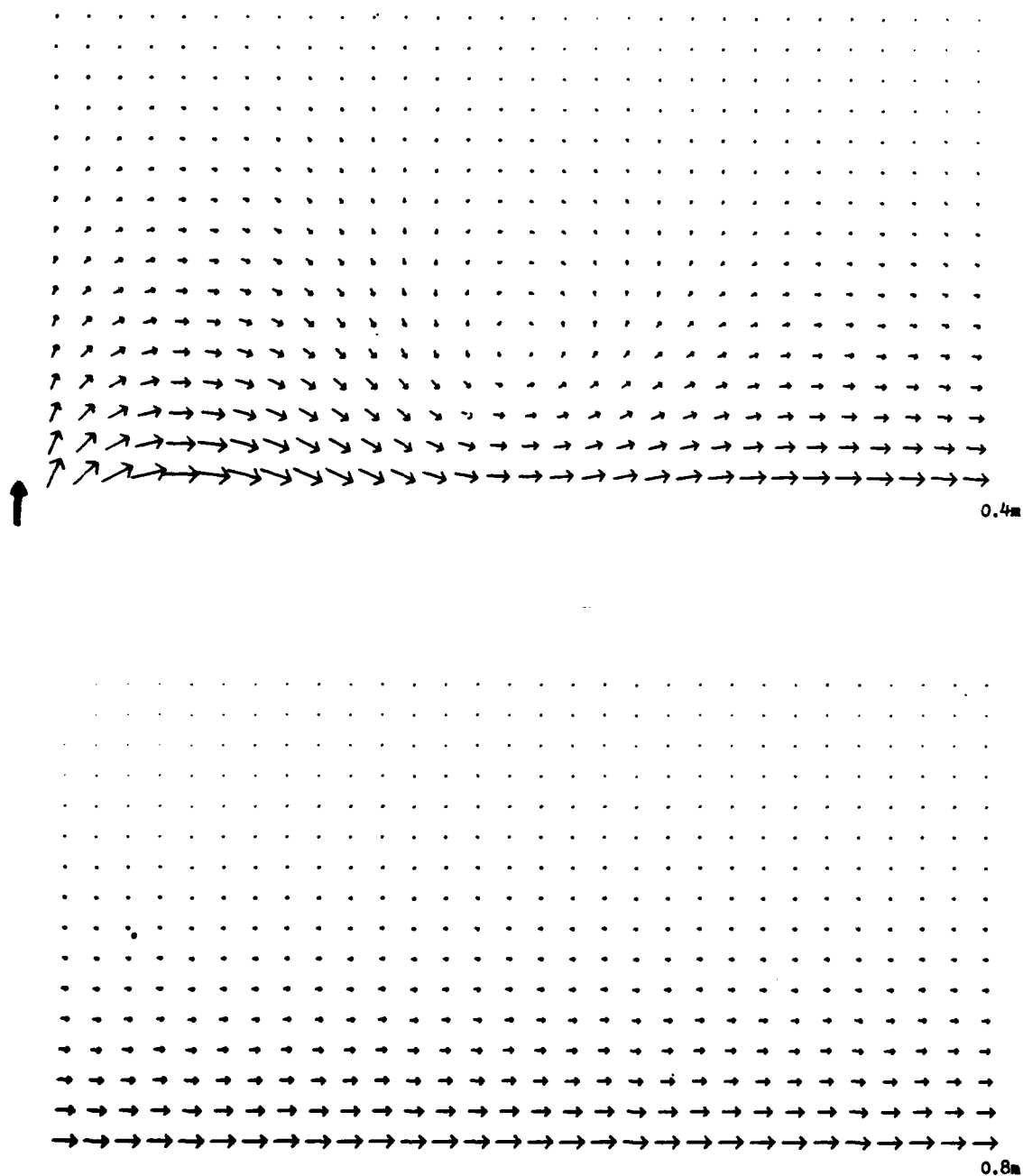


FIG.4 INTENSITY VECTOR PLOT. FORCE EXCITATION 1kHz

TWO 1CM STEEL PLATES SEPARATED BY 20CM WATER

FREQUENCY=1000HZ

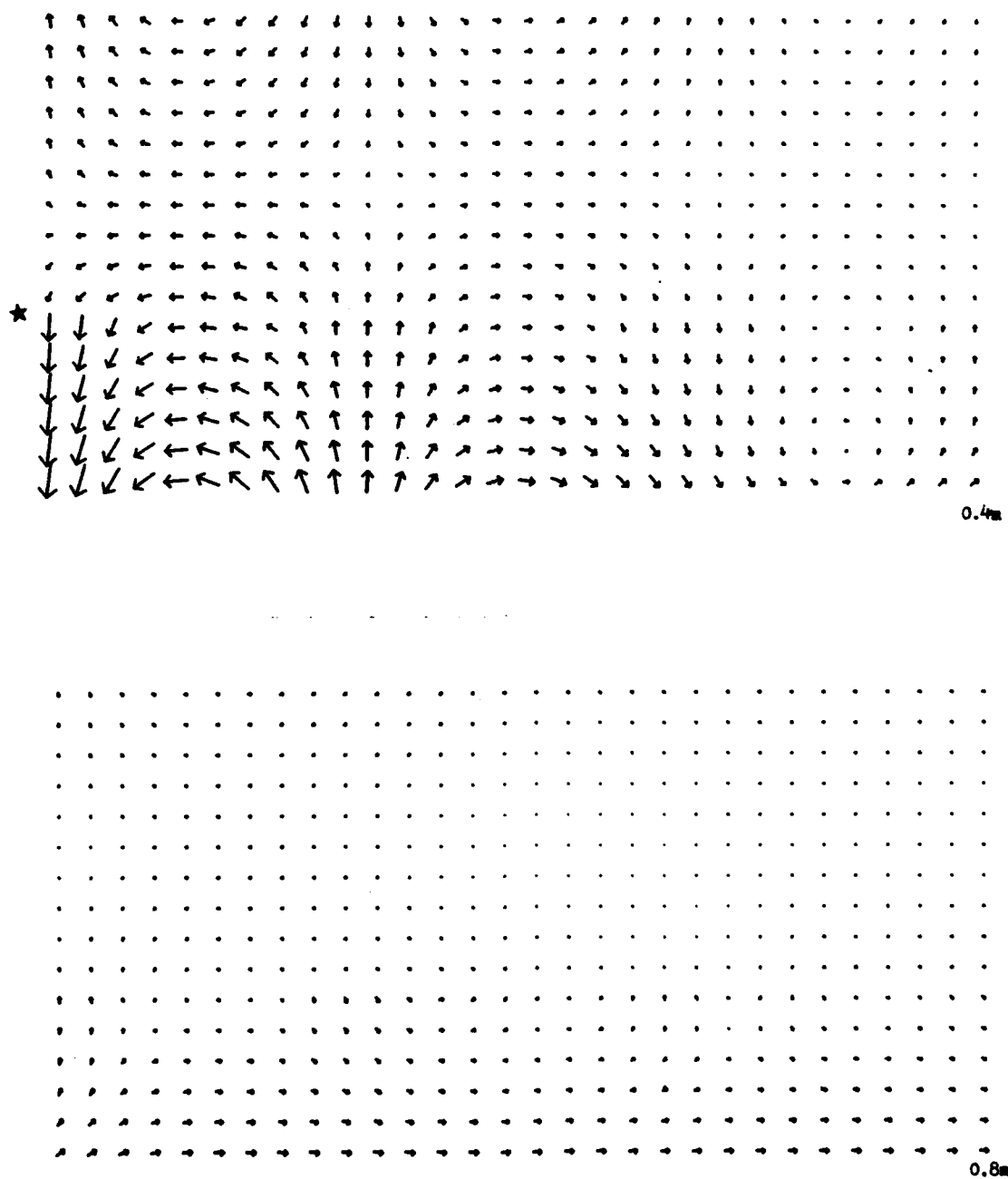


FIG.5 INTENSITY VECTOR PLOT. SOURCE EXCITATION 1kHz

TWO 1CM STEEL PLATES SEPARATED BY 20CM WATER

FREQUENCY=4000HZ

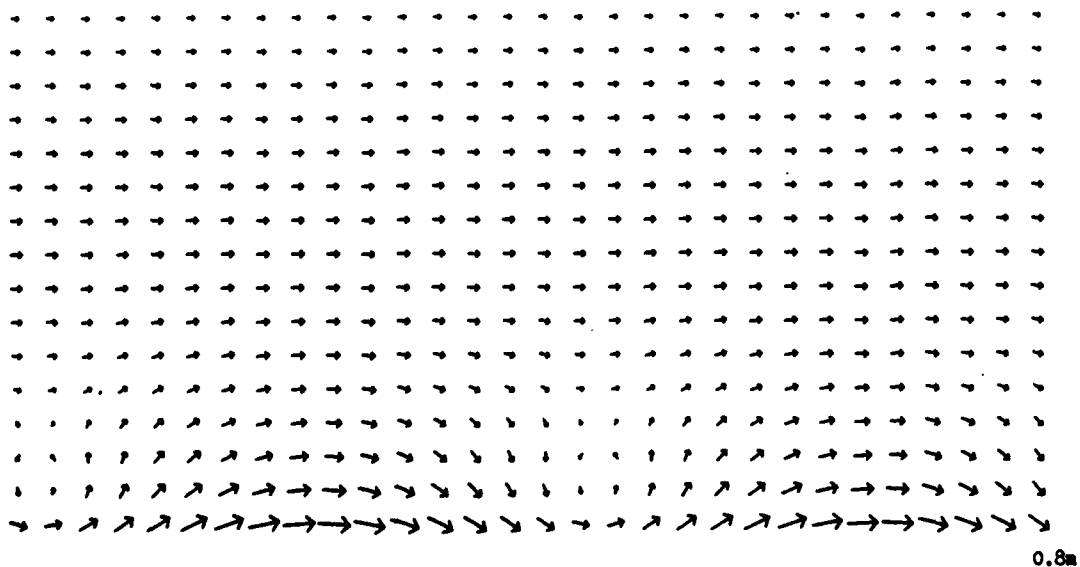
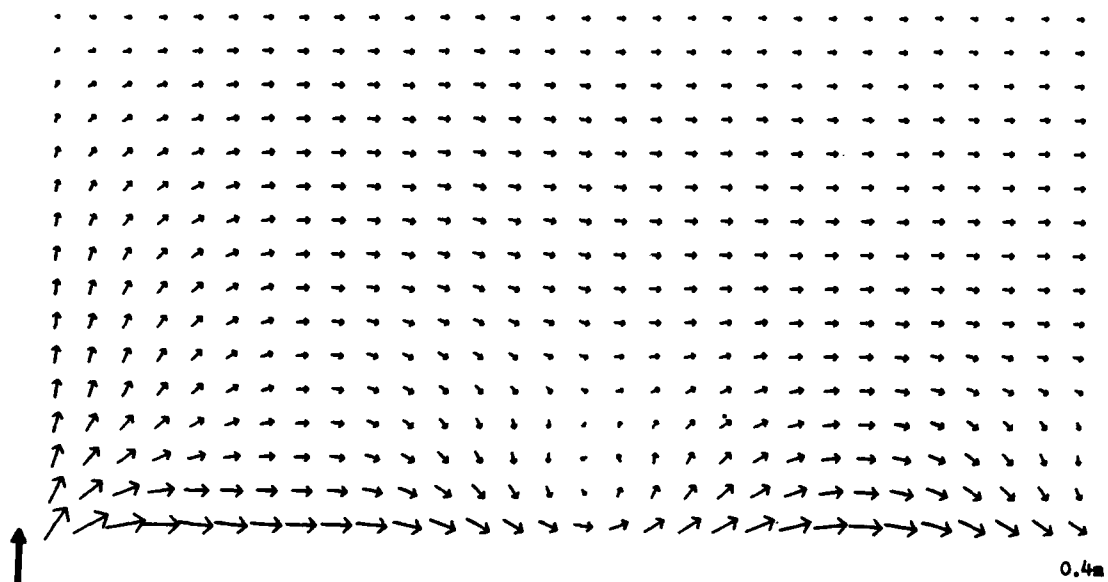


FIG.6 INTENSITY VECTOR PLOT. FORCE EXCITATION 4kHz

TWO 1CM STEEL PLATES SEPARATED BY 20CM WATER

FREQUENCY=4000HZ

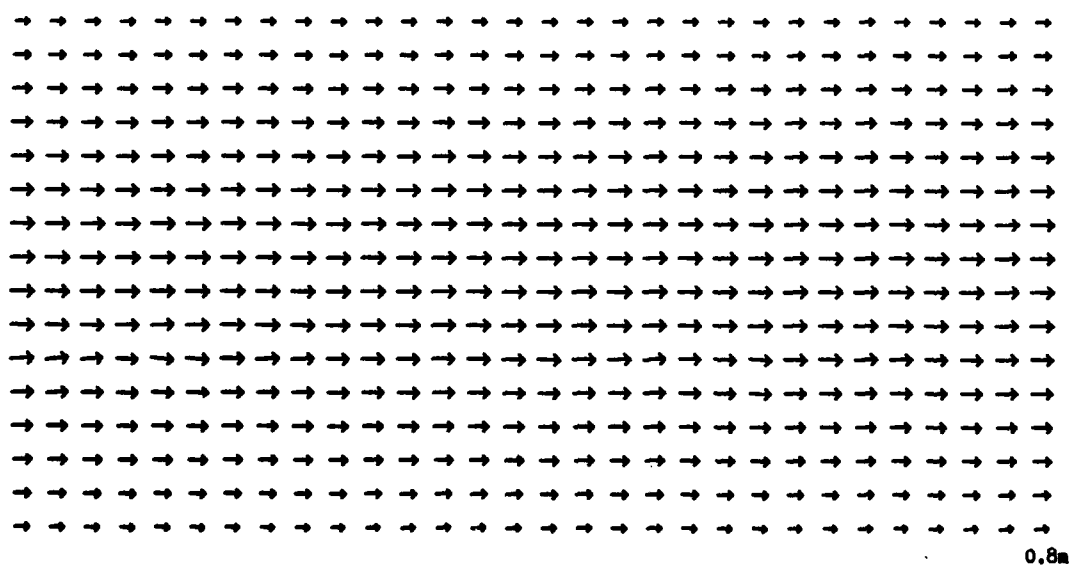
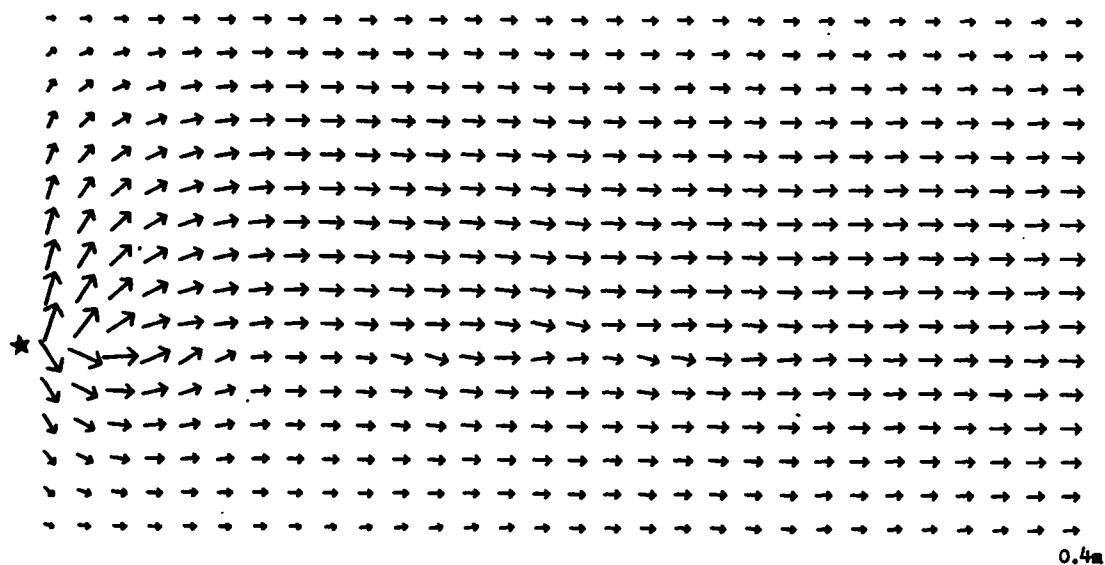


FIG.7 INTENSITY VECTOR PLOT. SOURCE EXCITATION 4kHz

TWO 1CM STEEL PLATES SEPARATED BY 20CM WATER

FREQUENCY=7000HZ

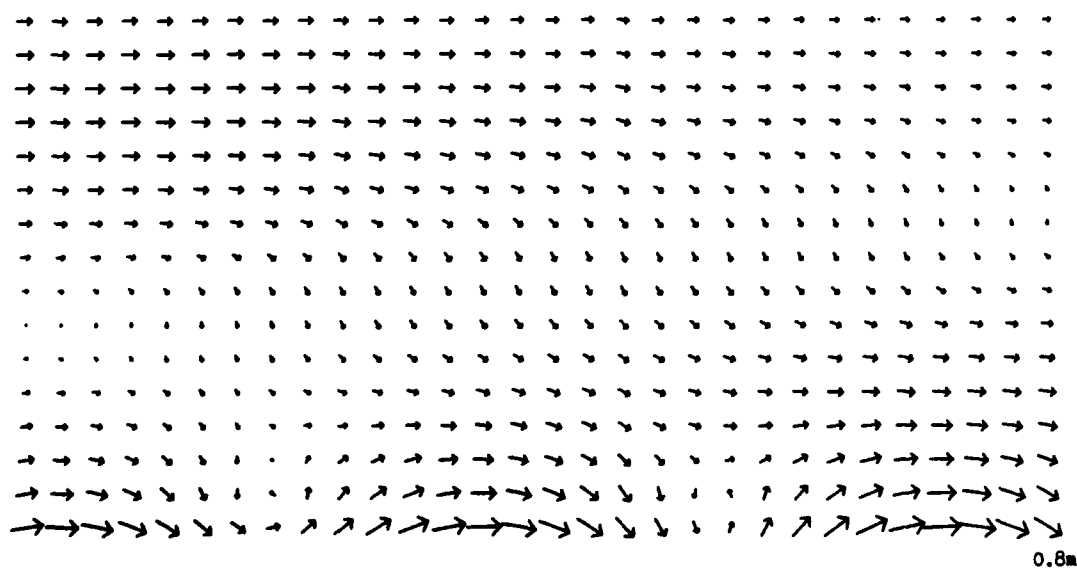
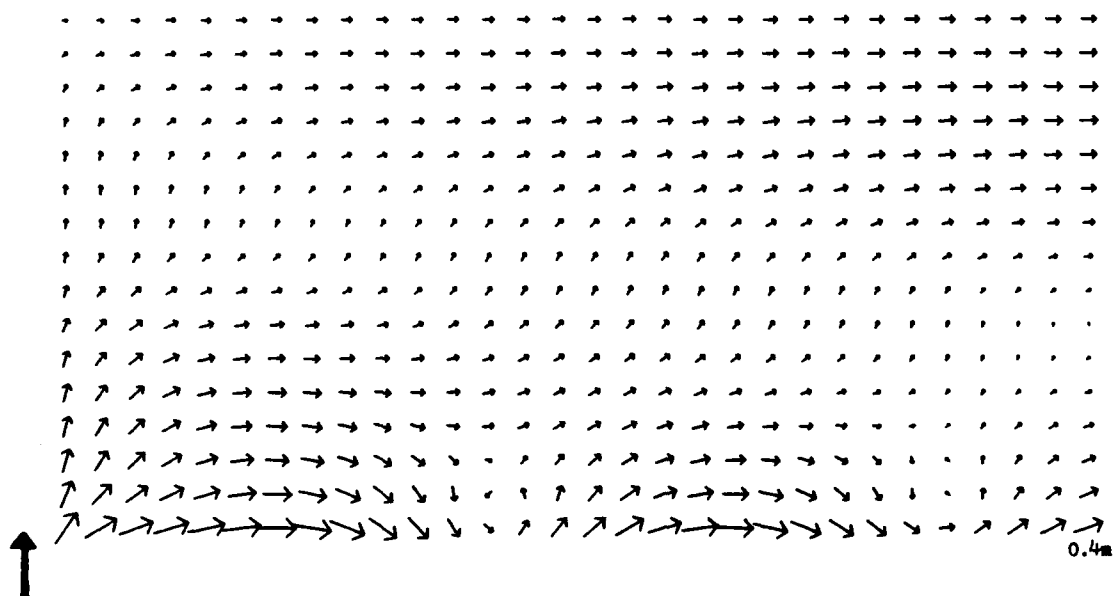
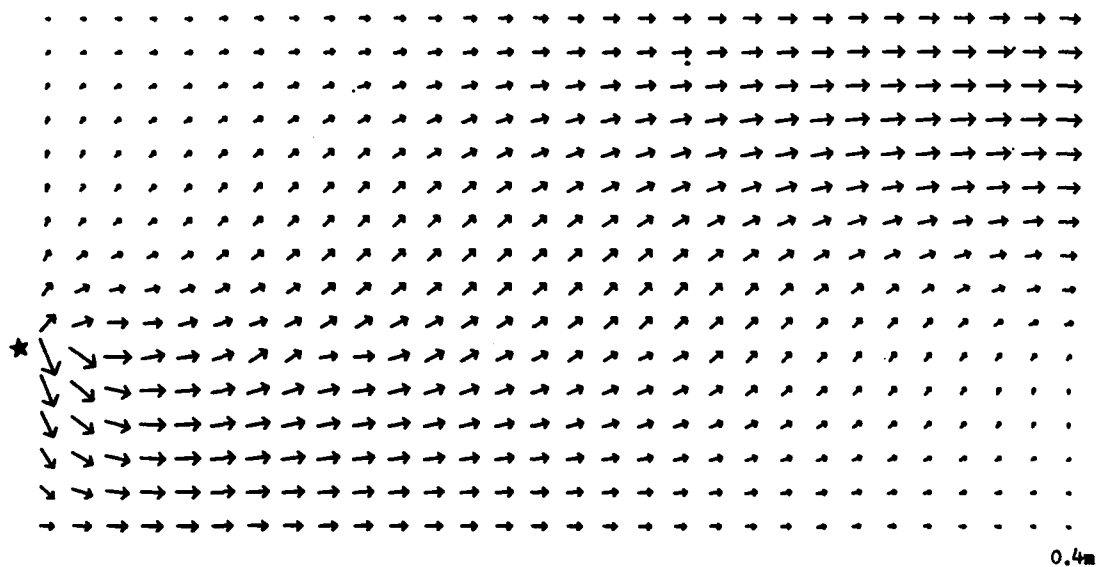


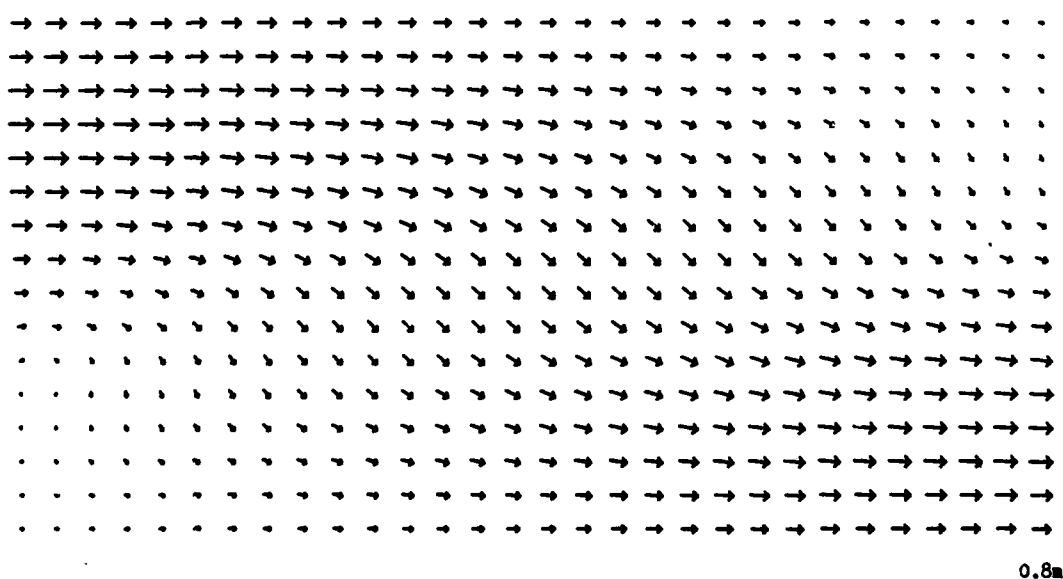
FIG.8 INTENSITY VECTOR PLOT. FORCE EXCITATION 7kHz

TWO 1CM STEEL PLATES SEPARATED BY 20CM WATER

FREQUENCY=7000HZ



0.4m



0.8m

FIG.9 INTENSITY VECTOR PLOT. SOURCE EXCITATION 7kHz

TWO 1CM STEEL PLATES SEPARATED BY 20CM WATER

FREQUENCY=10000HZ

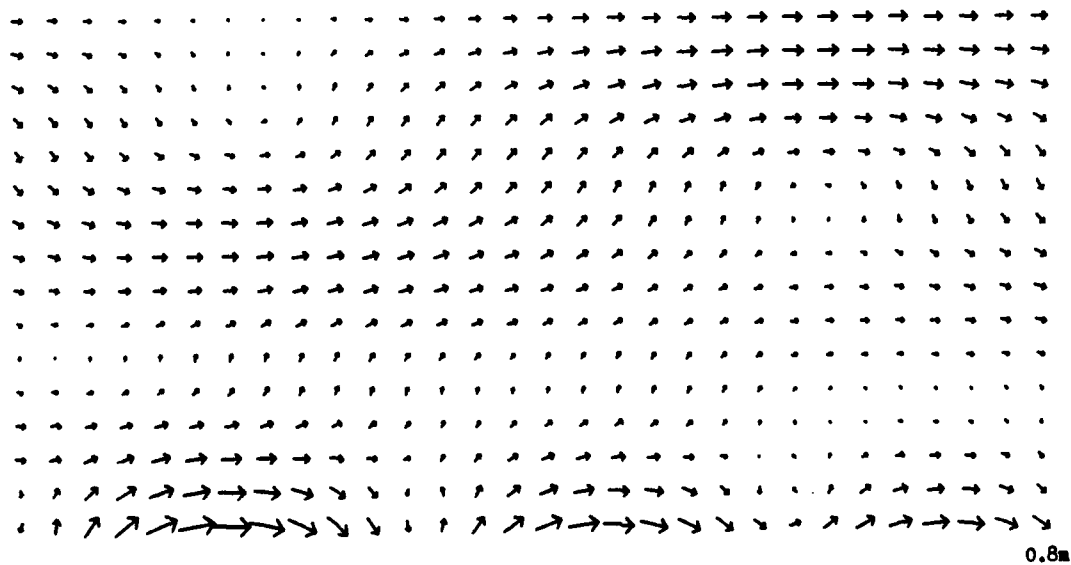
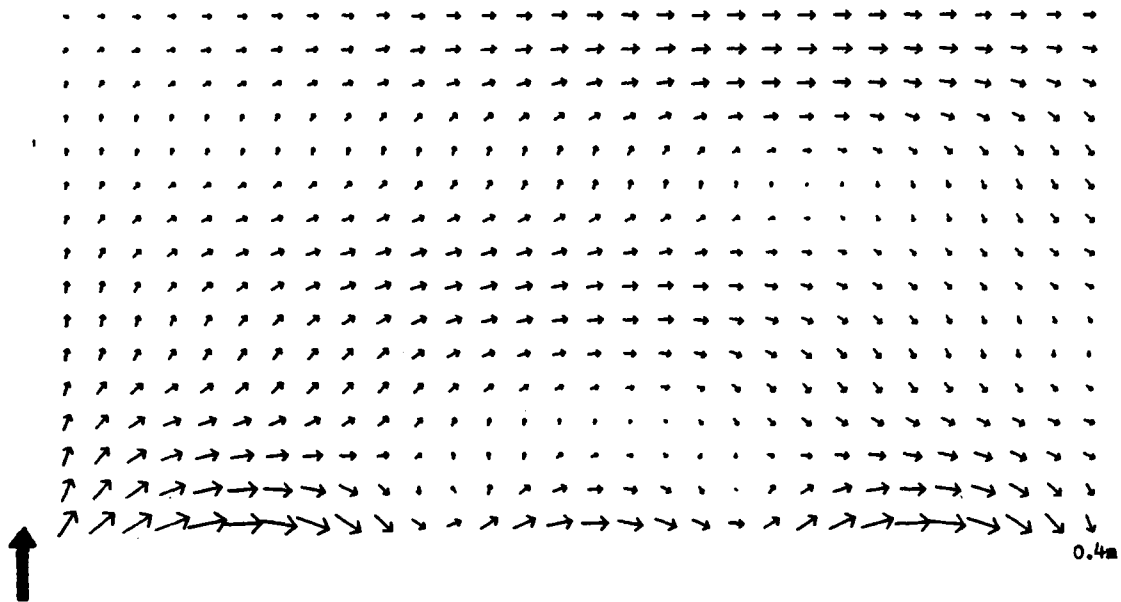


FIG.10 INTENSITY VECTOR PLOT. FORCE EXCITATION 10kHz

UNLIMITED

TWO 1CM STEEL PLATES SEPARATED BY 20CM WATER

FREQUENCY=10000HZ

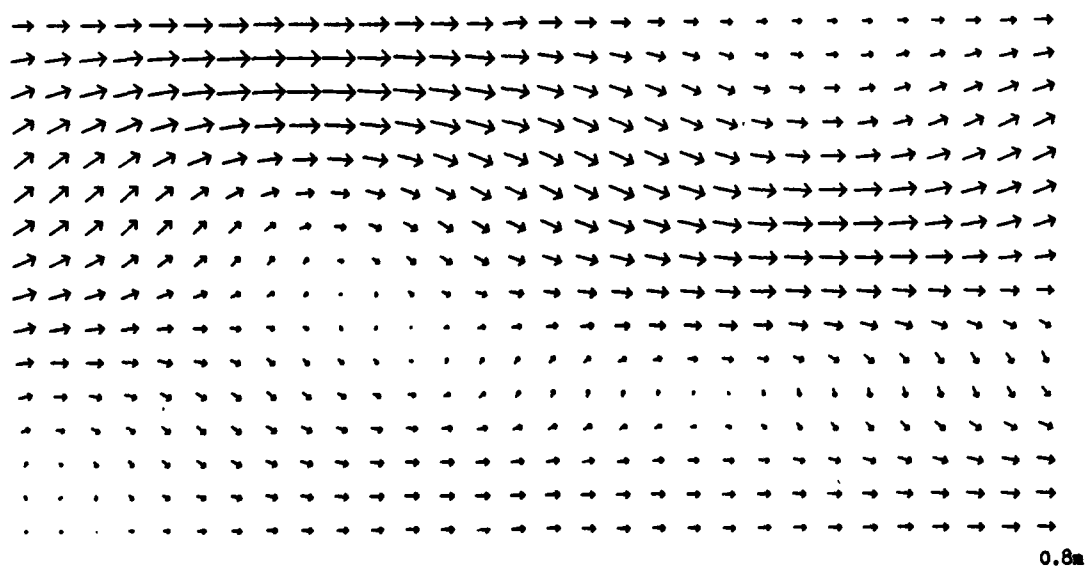
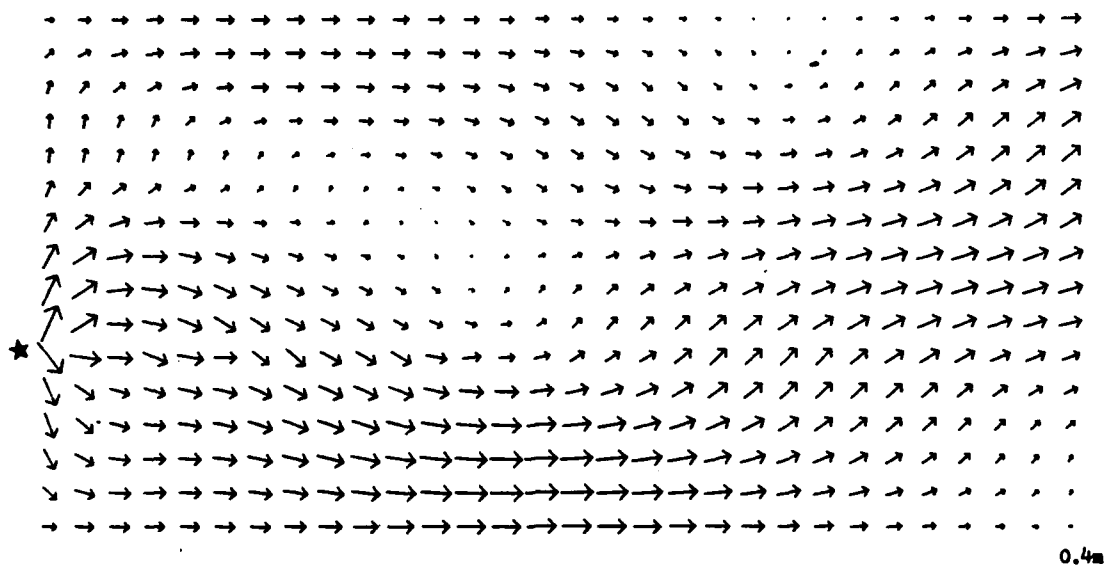


FIG.11 INTENSITY VECTOR PLOT. SOURCE EXCITATION 10kHz

DISTRIBUTION

Copy No

DGRA/CS(RN)/DNA

1

DAUWE

2

DES Washington

3

CS(R) 2e (Navy)

4

CNA AD/SR

5

DRIC

6-45

ARE (Teddington) File

46-53

ARE (Teddington) Mr J H James

54

ARE (Teddington) Division N1 File

55

END

FILMED

9-84

DTIC